Boron-rich plasma by high power impulse magnetron sputtering of lanthanum hexaboride

Efim M. Oks[1] and André Anders[1*]

[1] State University of Control Systems and Radioelectronics, Tomsk, Russia

[2] Lawrence Berkeley National Laboratory, Berkeley, California, USA

*Corresponding Author.
        Dr. Andre Anders
        Lawrence Berkeley National Laboratory
        1 Cyclotron Road, MS 53
        Berkeley, CA 94720, USA
        Tel. +1-510-486-6745
        Fax +1-510-486-4374
        aanders@lbl.gov

1

Abstract

Boron-rich plasmas have been obtained using a LaB_6 target in a high power impulse sputtering (HiPIMS) system. The presence of $^{10}B^+$, $^{11}B^+$, Ar^{2+}, Ar^+, La^{2+} and La^+ and traces of La^{3+}, $^{12}C^+$, $^{14}N^+$, and $^{16}O^+$ have been detected using an integrated mass and energy spectrometer. Peak currents as low as 20 A were sufficient to obtain plasma dominated by $^{11}B^+$ from a 5 cm planar magnetron. The ion energy distribution function for boron exhibits an energetic tail extending over several 10 eV, while argon shows a pronounced peak at low energy (some eV). This is in agreement with models that consider sputtering (B, La) and gas supply (from background and "recycling"). Strong voltage oscillations develop at high current, greatly affecting power dissipation and plasma properties.

* * *

High power impulse magnetron sputtering (HiPIMS) is an emerging technology for plasma-assisted deposition of thin films.[1-4] In contrast to more conventional forms of sputtering, a significant fraction of sputtered target becomes ionized when traveling from the target toward the substrate. Some target ions participate in the sputtering process (self-sputtering) and others may reach the substrate where they are available for target cleaning/etching and self-ion-assisted deposition. Over the last decade, a great number of studies have been published on HiPIMS plasmas with metal cathodes operating in pure noble and reactive gas environments, and in a few cases in vacuum, i.e. in the "gas" of sputtered atoms only.[5] The field of HiPIMS was recently reviewed[1-4] and therefore there is no need here to dwell deeply on HiPIMS physics and general operation except pointing out very recent observations of traveling ionization zones.[6-9] Ionization zones are critical in the explanation of the observed high "anomalous" discharge current, the surprisingly high likelihood of ionization for sputtered ions and other features.[7]

With very few exceptions, HiPIMS studies made use of elemental targets. Among the exceptions, Macak et al.[10] (one of the very first papers on HiPIMS) sputtered a TiAl target, Alami et al.[11] used a Ti_3SiC_2 compound target to deposit Ti-Si-C thin films, Sarakinos et al.[12] demonstrated the use of a titanium suboxide target for HiPIMS, and Horstmann et al.[13] used an indium-tin-oxide (ITO) target to obtain transparent conducting films. In this work, we use a LaB_6 target, i.e., a target having a very light (B) and a very heavy (La) element. LaB_6 is a conducting, refractory ceramic with a high melting temperature of 2210°C. It is known as an exceptional thermionic electron emitter, even when sputter-deposited as a film.[14] Its low work function of about 2.6 eV can be beneficial to various types of discharges since an ample supply of secondary electrons ensures the necessary energy supply to the discharge. LaB_6 was primarily selected for its very large fraction of boron, an element of many uses. Although it has been demonstrated that pure boron can be used in HiPIMS discharges,[15] working with pure boron targets is difficult. First, the electrical conductivity at room temperature is insufficient for HiPIMS unless a high target temperature of 600°C or higher is used. Second, thermal stresses tend to fracture the target when cycling it to and from elevated temperature. In this contribution we report about experiments using a LaB_6 target. We focus on the discharge behavior and resulting plasma composition. We will show that boron-rich plasma can readily be obtained.

HiPIMS experiments were done in a 1-m diameter stainless steel vacuum chamber equipped with a cryogenic vacuum pump leading to a base of pressure about 10^{-4} Pa. The maximum pumping speed of 1200 l/s could be throttled through an adjustable valve, and the argon gas supply could be regulated up to 100 sccm with a mass flow controller. A 5 cm (2 inch) magnetron was used for the experiments; the LaB_6 target was 3.12 mm (1/8 inch) thick. The HiPIMS discharge was fed by a custom power supply essentially consisting of a 2 μF high voltage capacitor and a 0.8 mH series inductance made from large air-core coils. The capacitor could be charged up to 3 kV. The HiPIMS current pulses were started using a thyristor switch. A small (20 mA) direct current (dc) was superimposed by using a dc power supply (Glassman, maximum 3 kV) via a 4 kΩ series resistor in order to promote fast and reproducible HiPIMS pulse ignition. The dc and HiPIMS circuits were joined by high-voltage high-current diodes to prevent that one part of the circuit damages the other. The target potential was measured using a 100:1 voltage divider (Tektronix P5100) and the pulse current was determined by a current transformer (Pearson model 101, sensitivity 0.01 V/A, bandwidth 0.25 Hz - 4 MHz) while the dc current was simply read at the dc power supply's meter. All pulsed data were recorded with a 4-channel fast digital oscilloscope (Tektronix). Most experiments reported here were done in argon at 0.5 Pa as measured by a capacitance manometer (Baratron by MKS). The magnetron was facing a combined mass and energy spectrometer of the type EQP 300 by Hiden Ltd, with a target-analyzer distance of 10 cm. This instrument can measure plasma particles with a mass up to 300 amu and ion energy distribution functions up to 1 keV. The EQP 300 was used to determine the plasma composition under different discharge conditions. The following main ion isotopes were investigated for the various discharge conditions: $^{10}B^+$, $^{11}B^+$, Ar^{2+}, Ar^+, La^{2+} and La^+. Following a generally accepted protocol, the Hiden instrumental parameters were tuned for each ion species to reach maximum detector signal. To obtain information on the ion composition in the plasma, each ion energy distribution function was integrated over the ion energy, considering all different charge states and isotopes of the element of interest.

An LC-circuit with a thyristor results in a half-sine current pulse shape provided that the load (plasma) impedance is equal to or smaller than $\sqrt{L/C}$. The anode-cathode (target) voltage self-adjusts according to the plasma's impedance. LaB_6 has a relatively low electrical resistivity at room temperature ($1.6 \times 10^{-3}\,\Omega\,cm$) and therefore high discharge currents can be reached like with a metal target.

If a too high voltage was initially applied to the target, the discharge tends to arc. Modern commercial HiPIMS supplies suppress arcing by terminating the discharge as soon as the arc is detected. However, in our case, using a simple switched L-C circuit without arc suppression, arcs do occur initially practically with each discharge pulse, and therefore a procedure for target conditioning needed to be adopted. Short arcing events at relatively low applied voltage (300-400 V) condition the target by eroding preferred emission sites. As arcing events become less frequent, the voltage can gradually be increased beyond 500 V. After 10 to 15 minutes of conditioning with a pulse duration of 80 μs and a pulse repetition rate of 10 pulses per second, the system was conditioned from arcing with currents as low as 5 A to almost arc-free operation with peak currents of up to 200 A. The presence or absence of arcing can be readily recognized by measuring the target potential: as soon as arcing occurs, the target potential drops sharply to the typical arc voltage of just 20-30 V. For stable operation, the measurements of the IEDF were limited to peak currents up to 120 A after conditioning.

Figure 1 shows the pulse shapes of discharge voltage and current for peak currents of 50, 80 and 120 A. The approximately half-sinusoidal current pulse form is given by the LC-circuit of the power supply in conjunction with the impedance of the discharge. The examples were selected to show (a) how greatly the current can be increased with a rather small increase in voltage; and (b), how strongly voltage oscillations develop when the current is high. Those oscillations are more or less regular, especially near the current peak when the plasma impedance is lowest. Fast Fourier transform analysis revealed a peak in the power spectrum at about 385 kHz for 20 A, 705 kHz for 50 A, 835 kHz for 80 A, 910 kHz for 120 A (Fig. 2). The amplitude of voltage oscillations increases nonlinearly with increasing peak current and can exceed the average voltage for currents greater than 120 A (Figs. 1 and 2). Oscillations are indicators for plasma instabilities, and HiPIMS discharges are known to exhibit a wealth of waves and instabilities,[4,16] as do all $\mathbf{E} \times \mathbf{B}$ discharges.[17] The voltage cut off at about -125 V, clearly visible in the 120 A example, is not an artifact. A similar cutoff, albeit about at potential near zero, was also observed in other experiments,[18] however, the explanation invoking the "emergence of emission sites" seems not substantiated. Further research is needed.

Figure 3 shows the ion energy distribution functions for the most prominent ion species, $^{40}Ar^+$ and the boron isotope $^{11}B^+$, as well as $^{139}La^+$ for discharges with 80 A peak current. One can see that most argon ions are within 0-10 eV whereas the energy distribution for boron is composed of a narrow peak at low energy and a long tail, the latter containing most of the boron ions. The slope of the lanthanum distribution tail is different than the tail for boron since lanthanum has a lower sputtering yield, greater ionization rate and different transport features than boron. Significant amounts of La^{2+} and even traces of La^{3+} were recorded. Small amounts of $^{12}C^+$, $^{14}N^+$, and $^{16}O^+$ ions were also detected: they showed energy distributions similar to the argon distribution. The low energy peaks show shoulders and seem to be composed of sub-peaks or caused by temporary peak shifts. The latter is likely since the spectrometer entrance orifice was grounded at all times, whereas the plasma potential is known to shift during each pulse.[19,20]

Integrating over the ion energy distribution function and pulse length gives the number of ions of the specific type arriving at the detector. For each element, all ion charge states and isotopes, as applicable, were added in this procedure. The result is shown in Fig. 4 as a function of the discharge peak current. A peak current of zero means that the plasma was measured with the dc magnetron discharge only. As one should expect in this situation, the plasma is dominated by gas ions. Adding the HiPIMS pulse shifts the plasma composition towards of the target material. At a peak current of 10 A the number of argon and boron ions are about the same. The contribution of the gas is reduced to about 20% when a peak current of 50 A is reached. A high fraction of target ions implies self-sputtering, however, the plasma is never free of argon even as the peak current is further enhanced. This is consistent with the concept that the supply of gas atoms available for ionization stems not only from the background but includes "recycled" gas neutrals produced at the target by ion neutralization.[21]

In summary, we have demonstrated that HiPIMS with a LaB_6 target leads to plasma that is dominated by boron ions. A peak current as low as 20 A for a 5 cm diameter target was sufficient to produce boron-rich plasma. The fraction of argon remains about 20% even when the peak current is increased to 100 A and higher. The target potential exhibits strong oscillations, indicative for plasma instabilities, whose amplitude increases nonlinearly with peak current. The boron-rich plasma may be of use to applications where a fraction of lanthanum is desired or can be tolerated.

Figure Captions

Fig. 1 Voltage and current pulse shapes for a peak current of 50 A (top), 80 A (center), 120 A (bottom); 0.5 Pa argon.

Fig. 2 Average voltage, amplitude and typical frequency of oscillations as a function of the peak current; 0.5 Pa argon.

Fig. 3. Time-averaged ion energy distribution functions in the range 0-50 eV for $^{40}Ar^+$, $^{11}B^+$, and $^{139}La^+$, measured for 80 A peak current and 20 mA superimposed dc current; 0.5 Pa argon.

Fig. 4. Time-averaged plasma composition as a function of peak current; 0.5 Pa argon.

[1] A. Ehiasarian, in *Plasma Surface Engineering Research and its Practical Applications*, edited by R. Wei (Research Signpost, Kerala, India, 2008), p. 35.

[2] D. Lundin and K. Sarakinos, J. Mater. Res. **27,** 780 (2012).

[3] K. Sarakinos, J. Alami, and S. Konstantinidis, Surf. Coat. Technol. **204,** 1661 (2010).

[4] J. T. Gudmundsson, N. Brenning, D. Lundin, and U. Helmersson, J. Vac. Sci. Technol. A **30,** 030801 (2012).

[5] J. Andersson and A. Anders, Appl. Phys. Lett. **92,** 221503 (2008).

[6] A. Anders, P. Ni, and A. Rauch, J. Appl. Phys. **111,** 053304 (2012).

[7] A. Anders, Appl. Phys. Lett. **100,** 224104 (2012).

[8] A. P. Ehiasarian, A. Hecimovic, T. de los Arcos, R. New, V. Schulz-von der Gathen, M. Böke, and J. Winter, Appl. Phys. Lett. **100,** 114101 (2012).

[9] A. Kozyrev, N. Sochugov, K. Oskomov, A. Zakharov, and A. Odivanova, Plasma Physics Reports **37,** 621 (2011).

[10] K. Macák, V. Kouznetsov, J. Schneider, U. Helmersson, and I. Petrov, J. Vac. Sci. Technol. A **18,** 1533 (2000).

[11] J. Alami, P. Eklund, J. Emmerlich, O. Wilhelmsson, U. Jansson, H. Högberg, L. Hultman, and U. Helmersson, Thin Solid Films **515,** 1731 (2006).

[12] K. Sarakinos, J. Alami, and M. Wuttig, J. Phys. D: Appl. Phys. **40,** 2108 (2007).

[13] F. Horstmann, V. Sittinger, and B. Szyszka, Thin Solid Films **517,** 3178 (2009).

[14] S. J. Mroczkowski, J. Vac. Sci. Technol. A **9,** 586 (1991).

[15] V. I. Gushenets, A. Hershcovitch, T. V. Kulevoy, E. M. Oks, K. P. Savkin, A. V. Vizir, and G. Y. Yushkov, Rev. Sci. Instrum. **81,** 02B303 (2010).

[16] D. Lundin, U. Helmersson, S. Kirkpatrick, S. Rohde, and N. Brenning, Plasma Sources Sci. Technol. **17,** 025007 (2008).

[17] S. N. Abolmasov, Plasma Sources Sci. Technol. **21,** 035006 (2012).

[18] A. N. Odivanova, V. G. Podkovyrov, N. S. Sochugov, and K. V. Oskomov, Plasma Physics Reports **37,** 239 (2011).

[19] A. Rauch, R. Mendelsberg, J. M. Sanders, and A. Anders, J. Appl. Phys. **111,** 083302 (2012).

[20] A. Mishra, P. J. Kelly, and J. W. Bradley, J. Phys D: Appl. Phys. **44,** 425201 (2011).

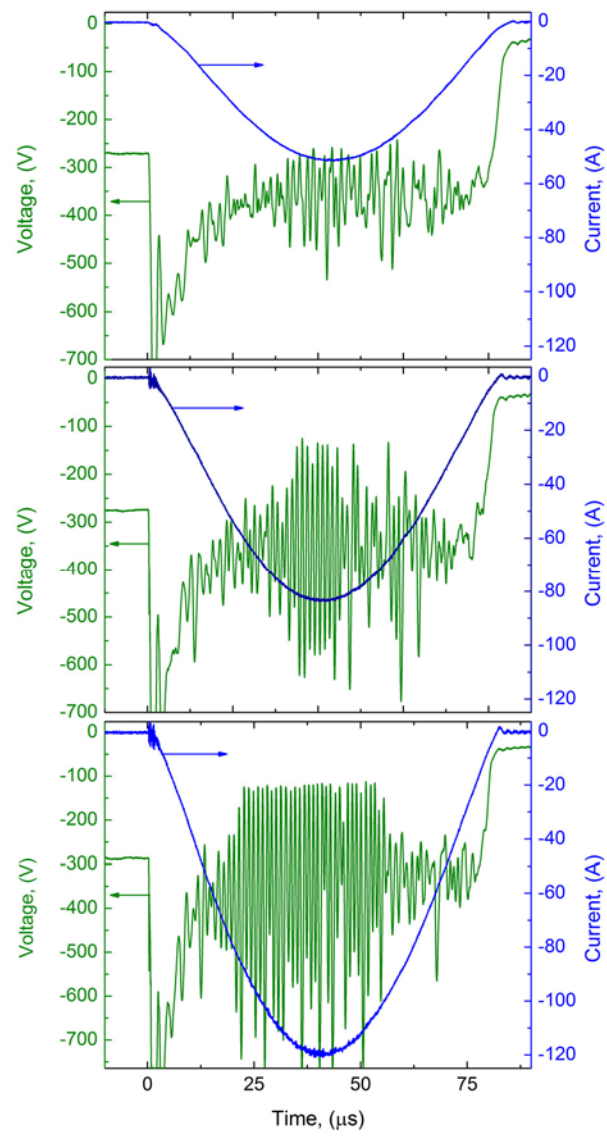[21] A. Anders, J. Čapek, M. Hála, and L. Martinu, J. Phys D: Appl. Phys. **45,** 012003 (2012).

Fig. 1

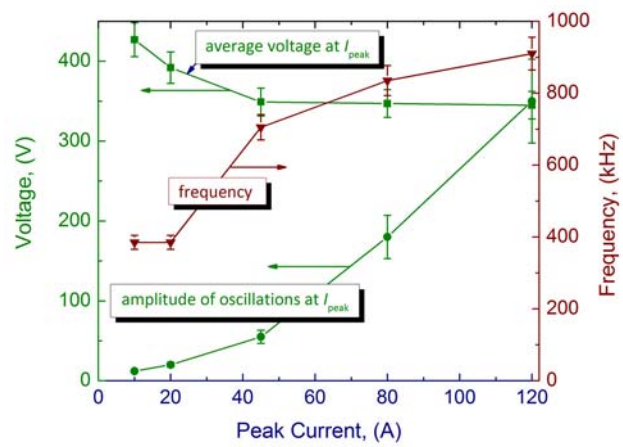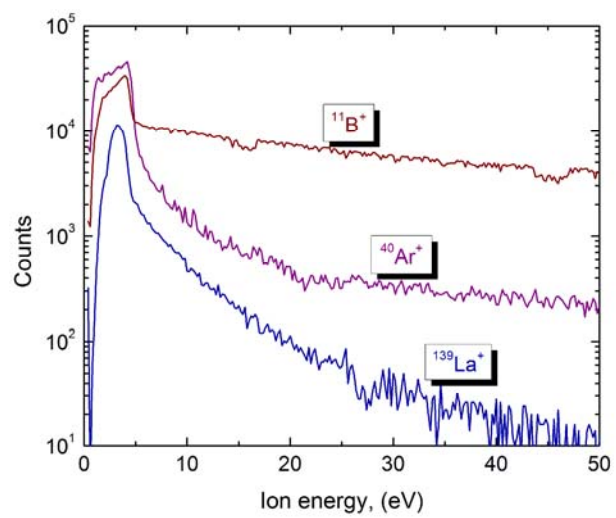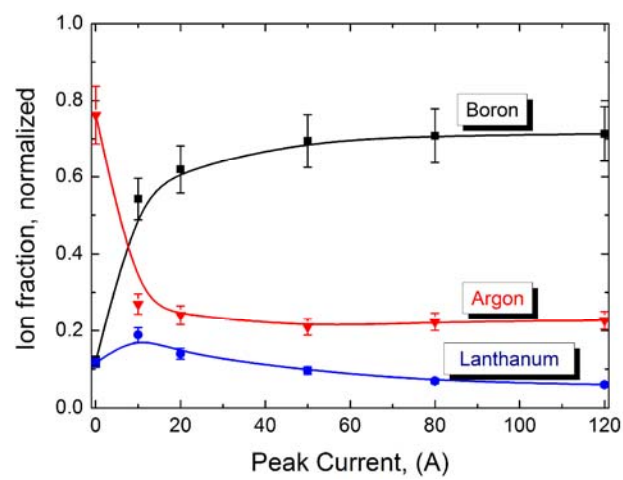Fig. 2

Fig. 3

Fig. 4